

# 1 **Designing Multi-model Applications with Surrogate Forecast Systems**

2 Leonard A. Smith<sup>1,2</sup>, Hailiang Du<sup>1,3</sup> and Sarah Higgins<sup>1</sup>

3 <sup>1</sup>Centre for the Analysis of Time Series,

4 London School of Economics, London WC2A 2AE. UK

5 <sup>2</sup>Pembroke College, Oxford, UK

6 <sup>3</sup>Department of Mathematical Sciences,

7 Durham University, Durham, UK

8 Email: [hailiang.du@durham.ac.uk](mailto:hailiang.du@durham.ac.uk)

## ABSTRACT

10 Probabilistic forecasting is common in a wide variety of fields including  
11 geoscience, social science and finance. It is sometimes the case that one has  
12 multiple probability-forecasts for the same target. How is the information in  
13 these multiple nonlinear forecast systems best “combined”? Assuming sta-  
14 tionarity, in the limit of a very large forecast-outcome archive, each model-  
15 based probability density function can be weighted to form a “multi-model  
16 forecast” which will, in expectation, provide at least as much information as  
17 the most informative single model forecast system. If one of the forecast  
18 systems yields a probability distribution which reflects the distribution from  
19 which the outcome will be drawn, Bayesian Model Averaging will identify  
20 this forecast system as the preferred system in the limit as the number of  
21 forecast-outcome pairs goes to infinity. In many applications, like those of  
22 seasonal weather forecasting, data are precious; the archive is often limited to  
23 fewer than  $2^6$  entries. In addition, no perfect model is in hand. It is shown  
24 that in this case forming a single “multi-model probabilistic forecast” can be  
25 expected to prove misleading. These issues are investigated in the surrogate  
26 model (here a forecast system) regime; where using probabilistic forecasts  
27 of a simple mathematical system allows many limiting behaviours of fore-  
28 cast systems to be quantified and compared with those under more realistic  
29 conditions.

## 30 **1. Introduction**

31 Forecasters are often faced with an ensemble of model simulations which are to be incorporated  
32 into quantitative forecast system and presented as a probabilistic forecast. Indeed, ensembles of  
33 initial conditions have been operational in weather centers in both the USA (Kirtman et al. 2014)  
34 and Europe (Palmer et al. 2004; Weisheimer et al. 2009) since the early 1990s and there is a  
35 significant literature on their interpretation (Raftery et al. 2005; Hoeting et al. 1999; Roulston  
36 and Smith 2003; Wang and Bishop 2004; Wilks 2006; Wilks and Hamill 2007). There is signifi-  
37 cantly less work on the design and interpretation of ensembles over model structures, although  
38 such ensembles are formed on weather (TIGGE (Bougeault et al. 2010)), seasonal (ENSEM-  
39 BLES (Weisheimer et al. 2009)) and climate (CMIP5 (Taylor et al. 2012)) forecast lead times.  
40 This paper focuses on the interpretation of multi-model ensembles in situations where data are  
41 precious, that is where the forecast-outcome archive is relatively small. Archives for seasonal  
42 forecasts fall into this category, typically limited to between 32 and 64 forecast-outcome pairs.<sup>1</sup>  
43 At times, the forecaster has only an “ensemble of convenience” composed by collecting forecasts  
44 made by various groups for various purposes. Alternatively, multi-model ensembles could be  
45 formed in collaboration using an agreed experimental design. This paper was inspired by the EN-  
46 SEMBLES project (Weisheimer et al. 2009), in which seven seasonal models were run in concert,  
47 with nine initial condition simulations under each model (Hewitt and Griggs 2004). Small-archive  
48 parameters<sup>2</sup> (SAP) forecast systems are contrasted with large-archive parameters (LAP) forecast  
49 systems using the lessons learned in experimental design based on the results originally reported  
50 by Higgins (2015).

---

<sup>1</sup>The observational data available for initialization and evaluation of the forecasts is very different before the satellite era.

<sup>2</sup>Here the parameters refer to the parameters involved in transforming multi-model ensemble into predictive distribution, for example the model weights, dressing and blending parameters (see Appendix A1) and they are estimated from an archive which is sometimes large and sometimes small.

51 We adopt the surrogate model context, taking relatively simple models of a chaotic dynamical  
52 system, then contrasting combinations of model to gain insight in how to build and test multi-  
53 model ensembles in a context where the data are not precious and a “perfect model” (the system)  
54 is known. In this context a robust experimental design can be worked out. There is, of course,  
55 an informal subjective judgement regarding how closely the consideration in the surrogate experi-  
56 ments map back into the real-world experiment. This is illustrated using a relatively simple chaotic  
57 dynamical system. Specifically, the challenges posed when evaluation data are precious are illus-  
58 trated by forecasting a simple one-dimensional system using four imperfect models. A variety  
59 of ensemble forecast system designs are considered: the selection of parameters and the relative  
60 value of “more” ensemble members from the “best” model are discussed. This consideration is  
61 addressed in a new generalization of the surrogate modeling framework (Smith (1992) and refer-  
62 ences therein); it is effectively a “surrogate forecasting system” approach, of value when practical  
63 constructions rule out the use of the actual forecast system of interest, as is often the case. In the  
64 large forecast-archive limit, the selection of model weights is shown to be straightforward and the  
65 results are robust as expected; when a unique set of weights are not well defined, the results remain  
66 robust in terms of predictive performance. It is shown that when the forecast-outcome archive is  
67 nontrivial but small, as it is in seasonal forecasting, uncertainty in model weights is large. The  
68 parameters of the individual model probabilistic forecasts vary widely between realizations in the  
69 SAP case; they do not do so in the LAP case. This does not guarantee that the forecast skill of SAP  
70 is significantly inferior to that of LAP, but it is shown that in this case the SAP forecast systems are  
71 significantly (several bits) less skillful. The goal of this paper is to refocus attention on this issue,  
72 not to claim to have resolved it. When evaluating models which push the limits of computational  
73 abilities of the day, one is forced to use systems simpler than those targeted by operational models  
74 to investigate ensemble forecasting. And whenever simplified models are employed, there is a

75 question as to whether the results hold in larger (imperfect) models. This question of “Even In Or  
76 Only In” (EIOOI) was discussed in Smith and Gilmour (1998).

77 Turning to the question of forming a multi-model forecast system, it is shown that (a) the model  
78 weights assigned given SAP are significantly inferior to those under LAP (and, of course, to the  
79 using ideal weights). (b) Estimating the best model in SAP is problematic when the models have  
80 similar skill. (c) Multi-model “out-of-sample” performance is often degraded due to the assign-  
81 ment of low (zero) weights to useful models. Potential approaches to this challenge (other than  
82 waiting for decades) are discussed. It is not possible, given the current archive, to establish the  
83 extent to which these results are relevant. The aim of the paper can only be to suggest a more  
84 general experimental design in operational studies which would identify or rule out the concerns  
85 quantified above. The paper merely raises a concern to which no exceptions are known, it does not  
86 attempt (nor could any paper today succeed) in showing this clear and present challenge to multi-  
87 model forecasting that dominates seasonal (or other) operational forecasts. It does, by considering  
88 well designed surrogate forecasting systems, provide insight into challenges likely to be faced by  
89 any multimodel forecast system of a design similar to the real forecast system of interest.<sup>3</sup>

---

<sup>3</sup>After reading this section, a reviewer asks if these results are relevant to readers of MWR? Consider the related question: what evidence is in hand that any approach is robust in operational models? Detailed questions of how large an ensemble should be or how a multi-model should be weighted (or even constructed (Du and Smith 2017)) can not be explored with operational models due to the extreme computational cost of such an evaluation. One could not evaluate, say, Figure 13 using operational models. The aim of surrogate modeling is to address such questions and demonstrate the robustness of the results for simpler target systems. The weakness of surrogate forecast systems is interpreting their relation of these results to those of operational systems of interest. The alternative is to have no well quantified and evaluated insight into the robustness at all. Were the results of Hide (1958) and Read (1992) useful to numerical weather forecasting? Were the many systems of mathematical equations constructed by Lorenz (1963, 1995)? Were the circuit studies on ensemble size by Machete and Smith (2016)? Surrogate forecast systems can aid in the design of operational test-beds and support their finding. The answer in our particular case appears to be that they are relevant.

## 90 2. From Ensemble(s) to Predictive Distribution

91 The ENSEMBLES project considered seasonal forecasts from seven different models; an initial  
92 condition ensemble of nine members was made for each model and launched four times a year (in  
93 the months of February, May, August and November). The maximum lead time was seven months,  
94 except for the November launch which extended to 14 months. Details of the project can be found  
95 in Alessandri et al. (2011); Doblas-Reyes et al. (2010); Weigel et al. (2008); Hewitt and Griggs  
96 (2004); Weisheimer et al. (2009); Smith et al. (2015).

97 The models are not exchangeable in terms of the performance of their probabilistic fore-  
98 casts. Construction of predictive functions via kernel dressing and blending with climatology  
99 (see Brocker and Smith (2008) and Appendix A1. for mathematical details) for each initial con-  
100 dition ensemble of simulations is discussed in Smith et al. (2015) (under various levels of cross-  
101 validation). Note that kernel dressing is not kernel density estimation (Silverman 1986); asked to  
102 suggest a reference that clarifies this common confusion of the two procedures, Silverman replied  
103 “As for anything in print, this is like asking for something in print that says the earth is round  
104 rather than flat? (B. Silverman private communication, 12 Apr 2018 12:54:11). Kernel Dressing  
105 does aim to reproduce the imperfect-model distribution from which it was drawn; Kernel Density  
106 Estimation always and only attempts to reproduce the distribution from which the ensemble mem-  
107 bers were drawn. Throughout the current paper, skill is quantified with I.J. Good’s logarithmic  
108 score (Good 1952; Roulston and Smith 2002); this score is sometimes (and in this paper) referred  
109 to as Ignorance (IGN) (Roulston and Smith 2002). As noted in Smith et al. (2015); Du and Smith  
110 (2017), IGN is the only proper and local score for continuous variables (Bernardo 1979; Raftery  
111 et al. 2005; Brocker and Smith 2006), and is defined by:

$$S(p(y), Y) = -\log_2(p(Y)), \quad (1)$$

112 where  $Y$  is the outcome and  $p(Y)$  is the probability of the outcome  $Y$ . In practice, given  $K$  forecast-  
 113 outcome pairs  $\{(p_i, Y_i) \mid i = 1, \dots, K\}$ , the empirical average Ignorance score of a forecast system  
 114 is then

$$S_E(p(y), Y) = \frac{1}{K} \sum_{i=1}^K -\log_2(p_i(Y_i)), \quad (2)$$

115 In practice, the skill of a forecast system can be reflected by the Ignorance of the forecast system  
 116 relative a reference forecast  $p_{ref}$ :

$$S_{rel}(p(y), Y) = \frac{1}{K} \sum_{i=1}^K -\log_2[(p_i(Y_i))/p_{ref}(Y_i)]. \quad (3)$$

117 Climatological forecast (climatology) is a commonly used reference forecast in meteorology.

### 118 **3. Simple Chaotic System Models Pair**

119 Without any suggestion that probabilistic forecasting of a one-dimensional chaotic map reflects  
 120 the complexity or the dynamics of seasonal forecasting of the Earth System, this paper draws  
 121 parallels. Parallels between challenges to probabilistic forecasting of scalar outcomes using mul-  
 122 tiple models with different structural model errors and a small forecast-outcome archive in low-  
 123 dimensional systems and those in high-dimensional systems. These challenges occur both in low-  
 124 dimensional systems and in high-dimensional systems. Whether or not suggestions inspired by  
 125 the low-dimensional case below generalize to high-dimensional cases (or other low-dimensional  
 126 cases, for that matter), would have to be evaluated on a case-by-case basis. The argument be-  
 127 low is that the challenges themselves can be expected in high-dimensional cases, leading to the  
 128 suggestion that they should be considered in the design of all multi-model forecast experiments.

129 The system to be forecast throughout this paper is the Moran-Ricker Map (Moran 1950; Ricker  
 130 1954) given in Equation 4. Selection of a simple, mathematically defined system allows the option  
 131 of examining the challenges of a small forecast-outcome archive in the context of results based on

132 very large archives. This is rarely possible for a physical system (see however Machete (2007);  
 133 Smith et al. (2015)). In this section the mathematical structure of the system and four imperfect  
 134 models of it are specified. The specific structure of these models reflects a refined experimental  
 135 design in light of the results of Higgins (2015).

136 Let  $\tilde{x}_t$  be the state of the Moran-Ricker Map at time  $t \in \mathbb{Z}$ . The evolution of the system state  $\tilde{x}$  is  
 137 given by

$$\tilde{x}_{t+1} = \tilde{x}_t e^{\lambda(1-\tilde{x}_t)}. \quad (4)$$

138 In the experiments presented in this paper,  $\lambda = 3$ , where the system is somewhat “less chaotic”  
 139 than using the value adopted in Sprott (2003) (Figure 1 shows the Lyapunov exponent as a function  
 140 of system parameter  $\lambda$  (Glendinning and Smith 2013)), in order to ease the construction of models  
 141 with comparable forecast skill. Define the observation at time  $t$  to be  $s_t = \tilde{x}_t + \eta_t$ , where the  
 142 observational noise,  $\eta_t$ , is independent and normally distributed ( $\eta_t \sim N(0, \sigma_{noise}^2)$ )<sup>4</sup>.

143 Four one-dimensional deterministic models are constructed, each one being an imperfect model  
 144 of the Moran-Ricker system. In the experiments presented here, the focus is on designing a multi-  
 145 model ensemble scheme and effective parameter selection for producing predictive distribution  
 146 from multiple models. Therefore the imperfect models as well as their parameter values are fixed.  
 147 These four models share the same state space as the system, and the observations are complete.  
 148 Note in practice, it is almost always the case that the model state  $x$  lies in a different space from  
 149 the system state  $\tilde{x}$ . The models are:

- 150 • **Model I**,  $G_1(x)$ , is built by first expanding the exponential term in Equation 4 to the 12<sup>th</sup>  
 151 order:

$$x_{t+1} = x(1 + \lambda(1-x) + \frac{1}{2!}(\lambda(1-x))^2 + \dots + \frac{1}{12!}(\lambda(1-x))^{12}). \quad (5)$$

---

<sup>4</sup>Observations are restricted to positive values.



152 The coefficient of each polynomial term is then truncated at the 3<sup>rd</sup> decimal place:

$$x_{t+1} = x(1 + 3(1-x) + 4.5(1-x)^2 + \dots + 0.004(1-x)^{11} + 0.001(1-x)^{12}). \quad (6)$$

153 • **Model II**,  $G_2(x)$ , is derived by first taking the logarithm of Equation 4 and expanding to the  
154 8<sup>th</sup> order:

$$\log x_{t+1} = \log x + \lambda - \lambda x = \log x + \lambda - \lambda e^{\log x} \quad (7)$$

$$\log x_{t+1} = -2\log x - \frac{3}{2!}(\log x)^2 - \frac{3}{3!}(\log x)^3 - \dots - \frac{3}{8!}(\log x)^8 \quad (8)$$

155 The coefficient of each polynomial term is then truncated at the 4<sup>th</sup> decimal place:

$$\log x_{t+1} = -2\log x - 1.5(\log x)^2 - 0.5(\log x)^3 - \dots - 0.0006(\log x)^7 - 0.0001(\log x)^8 \quad (9)$$

156 • **Model III**,  $G_3(x)$ , is obtained by expanding the right-hand side of Equation 4 in a Fourier  
157 series over the range  $0 \leq \tilde{x} \leq \pi$ . This series is then truncated at the 10<sup>th</sup> order to yield

$$x_{t+1} = \frac{a_0}{2} + \sum_{i=1}^{10} [a_i \cos(2ix_t) + b_i \sin(2ix_t)],$$

158 where the coefficients  $a_i$  and  $b_i$  are obtained by

$$a_i = \frac{2}{\pi} \int_0^\pi x e^{\lambda(1-x)} \cos(2ix) dx \quad (10)$$

$$b_i = \frac{2}{\pi} \int_0^\pi x e^{\lambda(1-x)} \sin(2ix) dx \quad (11)$$

159 • **Model IV**,  $G_4(x)$ , is obtained by expanding the right-hand side of Equation 4 by Laguerre  
160 Polynomials truncated at the 20<sup>th</sup> term.

$$x_{t+1} = \sum_{i=0}^{20} c_i L_i(x),$$

161 where  $L_i(x) = \sum_{k=0}^i \frac{(-1)^k}{k!} \binom{N}{k} x^k$  are the Laguerre Polynomials and the coefficients  $c_i$  are ob-  
 162 tained by

$$c_i = \int_0^{\infty} w(x) L_i(x) x e^{\lambda(1-x)} dx \quad (12)$$

163 with the weighting function  $w(x) = e^{-x}$ . Laguerre Polynomials are orthogonal and orthonor-  
 164 mal.

165 Notice that the order of the truncation for Model I, II, III and IV differ. These are chosen so that  
 166 each model represents the system dynamics well and the scales of their forecast skill are compa-  
 167 rable. Figure 2 plots the dynamical function of each model together with the system dynamics.  
 168 Figure 3 presents the histogram of the 1-step model error over 2048 different initial conditions  
 169 which are uniformly sampled between the minimum and maximum of the Moran-Ricker system.  
 170 It appears that Model I simulates the system dynamics well except when the initial condition is  
 171 near the maximum value of the system. For Model II, a large difference between the model dynam-  
 172 ics and the system dynamics appears only when the initial condition is near the minimum value  
 173 obtained by the system. Model III does not match the system dynamics well where  $x \gtrsim 1.5$  and  
 174 where the forward model reaches the maximum value of the map. Model IV matches the system  
 175 less well for initial conditions near the maximum value of the map.

176 Figure 4 plots the two-step model error for each model, while Figure 5 presents the histogram  
 177 of the 2-step model error. Generally, the structure of the model error is different. Different models  
 178 have different scales of model error in different local state space.

179 Again, there is, of course, no suggestion that the Moran-Ricker system resembles the dynamics  
 180 of the Earth. Rather, the framework presented here (and in Higgins (2015)) provides probabilistic  
 181 forecasts from structurally flawed models; the model-based forecasts (and ideal probabilistic fore-  
 182 casts formed using the perfect model) differ nontrivially from each other, and as the models are

183 nonlinear the forecast distributions are non-Gaussian. It is these challenges to multi-model fore-  
184 cast system development that are illustrated in this paper, which should (of course) not be taken to  
185 present an actual geophysical forecast system; indeed the verifications in the observational record  
186 rules out examination of LAP in geophysical systems, while computational requirements rule out  
187 extensive examination of SAP in “state-of-the-art” geophysical models.

## 188 **4. Ensemble Formation**

### 189 *a. Initial Condition Ensembles for Each Model*

190 In the experiments presented in this paper, each model produces ensemble forecasts by iterating  
191 an ensemble of initial conditions (IC). The initial condition ensemble (ICE) is formed by perturb-  
192 ing the observation with random draws from a Normal distribution,  $N(0, \kappa_\tau^2)$ . If the model were  
193 perfect and the observation were exact,  $\kappa_\tau$  would be zero; as neither of these conditions is met  
194 one does not expect  $\kappa_\tau$  to be zero. Such a perturbation parameter  $\kappa_\tau$  is chosen to minimize the  
195 Ignorance score at lead time  $\tau$ . When making medium-range forecasts, the European Centre for  
196 Medium-Range Weather Forecasts (ECMWF) selects a perturbation size such that the RMS error  
197 between the ensemble members and the ensemble mean at a lead time of two days is roughly equal  
198 to the RMS of the ensemble mean and the outcome at two days.

199 In the experiments presented below, each initial condition ensemble will contain  $N_e = 9$  mem-  
200 bers, following the ENSEMBLES protocol. Consider first the case of a large archive, with  
201  $N_a = 2048$ . For a given  $\kappa$  and lead time  $\tau$ , the kernel dressing and climatology-blend paramete-  
202 ter values are fitted using a training forecast-outcome archive which contains  $N_l = 2048$  forecast-  
203 outcome pairs. The Ignorance score is then calculated using an independent testing forecast-  
204 outcome set which contains  $N_t = 2048$  forecast-outcome pairs. Figure 6a shows the optimal per-

205 turbation parameter  $\kappa$  for each model varies with lead time.<sup>5</sup> The Ignorance score for each model  
206 at different lead time, using the values of  $\kappa$  in Figure 6a, is shown in Figure 6b. The sampling  
207 uncertainty across forecast launches is represented by a bootstrap resampling procedure, which  
208 resamples the set of forecast Ignorance scores for each model, with replacement. The bootstrap  
209 resampling intervals are shown as vertical bars in Figure 6 as a 5 – 95% interval. As seen in Figure  
210 6a, for each model, the preferred value of  $\kappa$  varies significantly (by about a factor of 2) between  
211 different forecast lead times. Defining a  $N_e$ -member forecast system requires selecting a specific  
212 value of  $\kappa$  for each model. In this paper, the value of  $\kappa$  for each model is chosen by optimizing the  
213 forecast Ignorance score at lead time 1. Sensitivity tests have been conducted and the Ignorance  
214 score at other lead times is much less sensitive to  $\kappa$  than that at lead time 1. Bias correction in the  
215 dressing blending approach is another concern. Hodyss et al. (2016) discussed bias in a real-world  
216 context. The dressing blending approach can be generalized by including a shifting parameter (see  
217 Brocker and Smith (2008)) to account for model bias. Including the shifting parameter does, in  
218 fact, improve the Ignorance score out-of-sample (in each model at almost all lead times) in this  
219 case. As the improvement is typically less than one 20th of a bit (sometimes zero), such shifting  
220 parameter is not included in the dressing blending throughout the experiments presented in the  
221 current paper.

## 222 *b. On the Number of IC Simulations in Each Ensemble*

223 Forecast system design relies on the knowledge of the relationship between the size of the fore-  
224 cast ensemble and the information content of the forecast (Smith et al. 2015). Usually, the cost of  
225 developing a brand new model is tremendously larger than the cost of increasing the number of

---

<sup>5</sup>As noted by a reviewer, there is uncertainty in the  $\kappa$  values reported in Figure 6a. To quantify this uncertainty, the estimate of  $\kappa$  was bootstrap resampled. The results (not shown) show variation in  $\kappa$ , at lead time 1 always less than 50%, but very little variation in the corresponding Ignorance value for each model.

226 ensemble members<sup>6</sup>. Furthermore the cost of increasing the ensemble size increases only (nearly)  
227 linearly and decreases as technology improves.

228 As the number of ensemble members increases, the true limitation due to structural model error  
229 becomes more apparent. Figure 7 shows that forecast Ignorance varies as ensemble size increases.  
230 Improvement from the additional ensemble members can be noted, especially at shorter lead times.

## 231 **5. Forecast System Design and Model Weighting When Data Are Precious**

### 232 *a. Forecasts With a Large Forecast-outcome Archive*

233 As  $N_a$ , the size of the forecast-outcome archive, increases, one expects robust results since large  
234 training sets and large testing sets are considered. To examine this, 512 different training sets are  
235 produced, each contains 2048 forecast-outcome pairs. For each archive, the kernel width  $\sigma$  and  
236 climatology-blend weight  $\alpha$  are fitted for each model's forecasts at lead time. Figures 8a and 8b  
237 show the fitted values of the dressing parameters and climatology-blend weights. The error bars  
238 reflect the central 90<sup>th</sup> percentile over 512 samples. The variation of the weight assigned to the  
239 model appears small. The variation of the fitted kernel width is small at short lead times and large  
240 at long lead times. Especially at lead time 5, the fitted value for Model IV has relatively large  
241 variation. This, however, does not indicate that the estimate is not robust but suggests the Ignorance  
242 score function in the parameter space is relatively flat near the minimum. To demonstrate  
243 this, the empirical Ignorance is calculated for each archive of kernel width and climatology-blend  
244 weight based on the same testing set (which contains another 2048 forecast-outcome pairs). Figure  
245 8c plots the Ignorance score and its 90<sup>th</sup> percentile as a function of lead time. Notice the 90<sup>th</sup>  
246 percentile ranges are always very narrow.

---

<sup>6</sup>And financially, the cost falls on the current account not the capital account.

247 The next two paragraphs echo Smith et al. (2015). There are many ways to combine multiple  
 248 single model forecast distributions into a single probabilistic (multi-model) forecast distribution  
 249 (Hagedorn et al. 2005; Brocker and Smith 2008). A simple approach is to treat each model equally  
 250 and therefore apply equal weight to each individual model (see, for example, Weisheimer et al.  
 251 (2009)). In general, different models perform differently in terms of forecasts, for example, the  
 252 ECMWF model significantly outperforms other models in seasonal forecasts (Smith et al. 2015).  
 253 Therefore, applying non-equal weights to all contributing models might provide more skillful  
 254 multi-model forecast distribution (see, for example, Rajagopalan et al. (2002)). Following Doblas-  
 255 Reyes et al. (2005) and Smith et al. (2015), define the combined multi-model forecast distribution  
 256 to be the weighted linear sum of the constituent distributions:

$$p_{mm} = \sum_i \omega_i p_i, \quad (13)$$

257 where  $p_i$  is the individual forecast distribution from the  $i^{th}$  model and  $\omega_i$  ( $\sum_i \omega_i=1$ ) the correspond-  
 258 ing weight. The weighting parameters  $\omega_i$  may be determined according to their performance in a  
 259 past forecast-outcome archive. The weights of individual models are expected to vary as a function  
 260 of lead time.

261 It is computationally costly and potentially results in ill-fitted model weights, if all the weights  
 262 are fitted simultaneously. To avoid both issues, a simple iterative approach (Du and Smith 2017)  
 263 is adopted. For each lead time, the best (in terms of Ignorance) model is first combined with the  
 264 second-best model to form a combined forecast distribution (by assigning weights to both models  
 265 that optimize the Ignorance of the combined forecast). The combined forecast distribution is then  
 266 combined with the third-best model to update the combined forecast distribution. This process  
 267 is repeated until inclusion of the “worst” model is considered. Note each time a new model is  
 268 included in the combined model, only two weights need to be assigned. Figure 8d shows the

269 weights assigned to each model as a function of lead time. The cyan line in Figure 8c shows the  
270 variation of the Ignorance score for the multi-model forecast given those estimated model weights  
271 is very small.

272 *b. Forecast With a Small Forecast-outcome Archive*

273 When given a small forecast-outcome archive (e.g. from a  $\sim 40$ -year seasonal forecast-outcome  
274 archive), one does not have the luxury of exploring a large collection of independent training and  
275 testing sets. Cross-validation is often approached by adopting a leave-one-out approach. The  
276 robustness of parameter fitting in such cases is of concern. To examine such robustness, a large  
277 number of forecast-outcome archives are considered. Each archive contains the same numbers of  
278 forecast-outcome pairs. For each archive, the parameter values are fitted via leave-one-out cross-  
279 validation. The distribution of fitted values over these small forecast-outcome archives is then  
280 compared with the fitted value from the  $N_a = 2048$  forecast-outcome archives above. Figure 9  
281 plots the histograms of the fitted climatology-blend weights given 512 forecast-outcome archives  
282 each containing  $N_a = 40$  forecast-outcome pairs. Notice that, in most cases, the distributions  
283 are very wide although they cover the value fitted given the large training set. There are some  
284 cases in which about 90 percent of the estimates are larger or smaller than the values fitted by  
285 the large archive, e.g. lead time 1 of Model I and Model II and lead time 4 of Model III and  
286 Model IV. It therefore appears that the robustness of fitting varies with lead time and the model.  
287 For shorter lead times, however, the weights are more likely to be over-fitted and, for longer lead  
288 times, the weights are more likely to be under-fitted. This is because at short lead times the model  
289 forecasts are relatively good; only a few forecast systems yield predictions that are worse than the  
290 climatological forecast. Small forecast-outcome archives, on the other hand, may not contain any  
291 model busts and so often overestimate the weights. The longer lead time case can be explained

292 similarly. Figure 10 plots the histogram of fitted kernel widths. Again, observe that there is much  
293 larger variation of the estimates here than when fitting with large forecast-outcome archives.

294 Poor estimation of the kernel width and climatology-blend weight will cause the forecast to  
295 lose skill and appear to underperform out-of-sample (due to inappropriately high expectations).  
296 This could, of course, be misinterpreted as climate change. For each of the 512 fitted kernel  
297 widths and climatology-blend weights, the Ignorance scores are calculated over the same testing  
298 set of 2048 forecast-outcome pairs. Figure 11 plots the histogram of the Ignorance score for each  
299 model. Using parameters fitted with small archives often results in significant degrading ( $\sim 1$  bit)  
300 of the Ignorance score of the forecasts. Correctly blending with the climatological distribution  
301 would yield a forecast score which, in expectation, is never worse than the climatology. When the  
302 blending parameter is determined using the small archive, however, the average relative Ignorance  
303 can be worse than climatology out-of-sample at long lead times (see for example in Figure 11).  
304 Figure 12 plots the histogram of multi-model weights. Clearly the variation of the model weights  
305 based on a small archive are much larger. Weights of zero are often assigned to model forecasts  
306 which contain useful information, for example.

## 307 **6. Multi-model vs Single Best Model**

308 As noted in Smith et al. (2015)<sup>7</sup>, it is sometimes said that a multi-model ensemble forecast is  
309 more skillful than any of its constituent single-model ensemble forecasts (see, for example, Palmer  
310 et al. (2004); Hagedorn et al. (2005); Bowler et al. (2008); Weigel et al. (2008); Weisheimer et al.  
311 (2009); Alessandri et al. (2011)). One common “explanation” (Weigel et al. 2008; Weisheimer  
312 et al. 2009; Alessandri et al. 2011) for this is that individual model tends to be overconfident  
313 with its forecast and a multi-model forecast reduces such overconfidence, which leads to a more

---

<sup>7</sup>These first two sentences are taken from Smith et al. (2015).



314 skillful forecast performance. As shown in Section 6, single model SAP forecast systems are  
315 typically between half a bit and two bits less skillful than a LAP system based on the same model.  
316 Can a SAP multi-model forecast system regain some of this potential skill? Figure 12 shows that  
317 this is unlikely, as the determination of model-weights given SAP varies tremendously relative to  
318 their LAP values. Again, it is the performance of the combination of weights that determine the  
319 skill of the forecasts, so this variation need not always be deadly.

320 Figure 13 shows the skill of the multi-model forecast system relative to the forecast system  
321 based on the single best model. Both the SAP and the LAP forecast systems show that the multi-  
322 model system usually outperforms the single model. Comparing SAP multi-model systems with  
323 the single best model SAP system (Figure 13b), the advantage of the multi-model system(s) is  
324 stronger when the best model (as well as all the parameters: model weights and dressing and  
325 climatology-blended parameters) are ill-identified. Comparing SAP multi-model systems with the  
326 single best model LAP system (Figure 13c), however, the advantage of the multi-model system(s)  
327 is weaker. Multi-model systems do **not** always outperform the single best model, especially at  
328 longer lead times.

329 At this point, one faces questions of resource distribution. A fair comparison of an N-model  
330 forecast system would be against a single model with n-times larger ensemble. (This, of course,  
331 ignores the operational fact that it is much more demanding to maintain an ensemble of models  
332 than to maintain a large ensemble under one model.) Secondly, note that for each model,  $\kappa$  was  
333 a function of lead time. At the cost of making ensemble members non-exchangeable, one could  
334 draw ensembles from distinct groups, and weight these members differently for each lead time.  
335 Finally, one could develop methods which treat the raw ensemble members from each of the  
336 models as non-exchangeable and use a more complex interpretation to form the forecast. While  
337 the simple forecast framework of this paper is an ideal place to explore such questions, they lie

338 beyond the scope of this paper. Instead, the extent to which the multi-model forecast system is  
339 more misleading than the single model systems concludes the discussion in the next section.

## 340 **7. Discussion and Conclusions**

341 A significant challenge to the design of seasonal probabilistic forecasting has been discussed  
342 and illustrated in a simple system where multiple models can easily be explored in long time  
343 limits. The challenge has been addressed within the surrogate modeling paradigm. In the actual  
344 system of interest, empirical data is precious: we have very few relevant out-of-sample forecasts,  
345 and doubling the current sample size will take decades. For these reasons we consider surrogate  
346 systems with sufficient similarity given the questions we wish to ask. We are forced to assume  
347 that the results obtained are general enough to make them informative for design in the real-  
348 world system; in this particular case we believe that they are: the challenges of interpreting small  
349 ensembles in any multi-model context are arguably quite similar. Similarly, the convergence to a  
350 clear conclusion in the limit of large ensembles is also arguably quite similar. The details of the  
351 rate at which information increases as the ensemble size increases will depend on the details of  
352 the dynamics of the system, the quality of the models, and so on. That said, there is sufficient  
353 evidence from the study above to show that some current multi-model ensemble studies do not  
354 employ initial condition ensembles of sufficient size to achieve robust results.

355 There is no statistical fix to the challenges of “lucky strikes” when a generally poor model  
356 places an ensemble member near an outcome “by chance”, and that particular outcome was not  
357 well predicted by the other forecast systems. Similarly “hard busts” in a small archive can distort  
358 the parameters of the forecast systems, when an outcome occurs relatively far from each ensemble  
359 member. In this case, wider kernels and/or heavier weighting on the climatology results. This  
360 may be due to structural model failure, or merely to a “rare” event, where rare is related to the

361 ensemble size. Given a sufficiently large ensemble, the forecast system could have assigned an  
362 (appropriately low) probability to the observed “bust” event.

363 In short, the brief duration of the forecast-outcome archive, typically less than 40 years in sea-  
364 sonal forecasting, limits the clarity both with which probability distributions can be derived from  
365 individual models and with which model weights can be determined. No clear solution to this  
366 challenge has been proposed, and while improvements on current practice can be made, it is not  
367 clear that this challenge can be met. Over long periods, like 512 years, the climate may not be well-  
368 approximated as stationary. In any event, both observational systems and the models themselves  
369 can evolve significantly on much shorter timescales, perhaps beyond recognition.

370 One avenue open to progress is in determining the relative skill of “the best model” (or a small  
371 subset) and the full diversity of models. Following Brocker and Smith (2008) it is argued that a  
372 forecast system under the best model with a large ensemble may well outperform the multi-model  
373 ensemble forecast system when both systems are given the same computer power. To test this in  
374 practice requires access to larger ensembles under the best model. This paper argues future studies,  
375 such as ENSEMBLES, could profitably adjust their experimental design to take this into account  
376 (see also Machete and Smith (2016)).

377 A second avenue is to reduce the statistical uncertainty of model fidelity within the available  
378 archive. This can be done by running large ensembles (much greater than “9”, indeed greater than  
379 might be operationally feasible) under each model. This would allow identification of which mod-  
380 els have significantly different probability distributions, and the extent to which they are (some-  
381 times) complementary. Tests with large ensembles also reveal the “bad busts” due to small en-  
382 semble size to be what they are. It can also suggest that those which remain are indeed due to  
383 structural model error.

384 In closing, it is suggested that perhaps the most promising way forward is to step away from the  
385 statistics of the ensembles, and consider the physical realism of the individual trajectories. One  
386 can look for shadowing trajectories in each model, and attempt to see what phenomena limit the  
387 model's ability to shadow. Identifying these phenomena, and the phenomena that cause them,  
388 would allow model improvement independent of the probabilistic skill of ensemble systems. This  
389 approach is not new, of course, but the traditional physical approach to model improvement which  
390 dates back to Charney. Modern forecasting methods do offer some new tools (Judd et al. 2008),  
391 and the focus on probabilistic forecasting is well placed in terms of prediction. The point here is  
392 merely that probabilistic forecast skill, while a sharp tool for decision support, may prove a blunt  
393 tool for model improvement when the data are precious.

## A1. From Simulation to a Predictive Distribution

This appendix is taken from Smith et al. (2015) Appendix A.

An ensemble of simulations is transformed into a probabilistic distribution function by a combination of kernel dressing and blending with climatology (Brocker and Smith 2008). An  $N$ -member ensemble at time  $t$  is given as  $X_t = [x_t^1, \dots, x_t^N]$ , where  $x_t^i$  is the value of a observable quantity for the  $i^{\text{th}}$  ensemble member. For simplicity, ensemble members given a model are considered exchangeable. Kernel dressing defines the model-based component of the density as:

$$p(y : X, \sigma) = \frac{1}{N\sigma} \sum_i^N K\left(\frac{y - (x^i)}{\sigma}\right), \quad (\text{A1})$$

where  $y$  is a random variable (the correspondent of the density function  $p$ ) and  $K$  is the kernel, taken here to be

$$K(\zeta) = \frac{1}{\sqrt{2\pi}} \exp\left(-\frac{1}{2}\zeta^2\right). \quad (\text{A2})$$

Thus each ensemble member contributes a Gaussian kernel centred at  $x^i$ . For a Gaussian kernel, the kernel width  $\sigma$  is simply the standard deviation determined empirically as discussed below.

Even for an ensemble drawn from the the same distribution as the outcome, there remains the chance of  $\sim \frac{2}{N}$  that the outcome lies outside the range of the ensemble. Given the nonlinearity of the model, such outcomes can be very far outside the range of the ensemble members. In addition to  $N$  being finite, the simulations are **not** drawn from the same distribution as the outcome, as the forecast system is never perfect in practice. To improve the skill of the probabilistic forecasts, the kernel dressed ensemble may be blended with an estimate of the climatological distribution of the system obtained by dressing the historical observations (see Brocker and Smith (2008) for more details, Roulston and Smith (2003) for alternative kernels and Raftery et al. (2005) for a Bayesian

414 approach). The blended forecast distribution is then written as

$$p(\cdot) = \alpha p_m(\cdot) + (1 - \alpha) p_c(\cdot), \quad (\text{A3})$$

415 where  $p_m$  is the density function generated by dressing the model ensemble and  $p_c$  is the estimate  
416 of the climatological density. The blending parameter  $\alpha$  determines how much weight is placed  
417 on the model. Specifying both values (kernel width  $\sigma$ , and climatology blended parameter  $\alpha$ )  
418 at each lead time defines the forecast distribution. Both parameters are fitted simultaneously by  
419 optimizing the empirical Ignorance score over the training set.

420 *Acknowledgments.* This research was supported by the LSE’s Grantham Research Institute on  
421 Climate Change and the Environment and the ESRC Centre for Climate Change Economics and  
422 Policy, funded by the Economic and Social Research Council and Munich Re; it was also sup-  
423 ported as part of the EPSRC-funded Blue Green Cities (EP/K013661/1). Additional support for  
424 H.D. was also provided by the EPSRC-funded Uncertainty analysis of hierarchical energy systems  
425 models: Models versus real energy systems (EP/K03832X/1) and Centre for Energy Systems In-  
426 tegration (EP/P001173/1). L.A.S. gratefully acknowledges the continuing support of Pembroke  
427 College, Oxford.

## 428 **References**

- 429 Alessandri, A., A. Borrelli, A. Navarra, A. Arribas, P. R. M. Déqué, and A. Weisheimer, 2011:  
430 Evaluation of probabilistic quality and value of the ensembles multi-model seasonal forecasts:  
431 Comparison with demeter. *Mon. Wea. Rev.*, **2**, 139.
- 432 Bernardo, J. M., 1979: Expected information as expected utility. *Ann. Stat.*, **7**, 686–690.
- 433 Bougeault, P., and Coauthors, 2010: The thorpex interactive grand global ensemble (tigge). *Bull.*  
434 *Amer. Met. Soc.*, **91**, 1059–1072.

- 435 Bowler, N. E., A. Arribas, and K. R. Mylne, 2008: The benefits of multi-analysis and poor-mans  
436 ensembles. *Mon. Wea. Rev.*, **136**, 4113–4129.
- 437 Brocker, J., and L. Smith, 2006: Scoring probabilistic forecasts: On the importance of being  
438 proper. *Wea. Forecasting*, **22**, 382–388.
- 439 Brocker, J., and L. Smith, 2008: From ensemble forecasts to predictive distribution functions.  
440 *Tellus A*, **60**, 663–678.
- 441 Doblas-Reyes, F. J., R. Hagedorn, and T. N. Palmer, 2005: The rationale behind the success of  
442 multi-model ensembles in seasonal forecasting. part ii: Calibration and combination. *Tellus A*,  
443 **57**, 234–252.
- 444 Doblas-Reyes, F. J., A. Weisheimer, T. N. Palmer, J. M. Murphy, and D. Smith, 2010: Forecast  
445 quality assessment of the ensembles seasonal-to-decadal stream 2 hindcasts. *Technical Memo-*  
446 *randum (ECMWF)*, 621.
- 447 Du, H., and L. Smith, 2017: Multi-model cross-pollination in time. *Physica D: Nonlinear Phe-*  
448 *nomena*, **353-354**, 31–38.
- 449 Glendinning, P., and L. Smith, 2013: Lacunarity and period-doubling. *Dynamical Systems*, **28**,  
450 111–121.
- 451 Good, I., 1952: Rational decisions. *J. R. Stat. Soc.*, 107–114.
- 452 Hagedorn, R., F. J. Doblas-Reyes, and T. N. Palmer, 2005: The rationale behind the success of  
453 multi-model ensembles in seasonal forecasting. part i: Basic concept. *Tellus A*, **57**, 219–233.
- 454 Hewitt, C. D., and D. J. Griggs, 2004: Ensembles-based predictions of climate changes and their  
455 impacts. *Eos, Transactions American Geophysical Union*, **85**, 566.

- 456 Hide, R., 1958: An experimental study of thermal convection in a rotating fluid. *Phil. Trans. R.*  
457 *Soc. Lond.*, 441–478.
- 458 Higgins, S., 2015: Limitations to seasonal weather prediction and crop forecasting due to non-  
459 linearity and model inadequacy. Ph.D. thesis, The London School of Economics and Political  
460 Science, London, UK.
- 461 Hodyss, D., E. Satterfield, J. McLay, T. M. Hamill, and M. Scheuerer, 2016: Inaccuracies  
462 with multimodel postprocessing methods involving weighted, regression-corrected forecasts.  
463 *Monthly Weather Review*, **144** (4), 1649–1668.
- 464 Hoeting, J., D. Madigan, A. Raftery, and C. Volinsky, 1999: Bayesian model averaging: a tutorial.  
465 *Stat. Sci.*, **14**, 382–417.
- 466 Judd, K., C. A. Reynolds, T. E. Rosmond, and L. A. Smith, 2008: The geometry of model error. *J.*  
467 *Atmos. Sci.*, **65**, 1749–1772.
- 468 Kirtman, B., and Coauthors, 2014: The north american multimodel ensemble: Phase-1 seasonal-  
469 to-interannual prediction; phase-2 toward developing intraseasonal prediction. *Earth Interac-*  
470 *tions*, **95** (4), 585–601, doi:10.1175/BAMS-D-12-00050.1.
- 471 Lorenz, E., 1995: Predictability: a problem partly solved. *Seminar on Predictability, 4-8 Septem-*  
472 *ber 1995*, ECMWF, Shinfield Park, Reading, ECMWF, Vol. 1, 1-18.
- 473 Lorenz, E. N., 1963: Deterministic nonperiodic flow. *Journal of the Atmospheric Sciences*, **20** (2),  
474 130–141.
- 475 Machete, R., 2007: Modelling a moore-spiegel electronic circuit: the imperfect model scenario.  
476 Ph.D. thesis, University of Oxford, UK.



- 477 Machete, R., and L. Smith, 2016: Demonstrating the value of larger ensembles in forecasting  
478 physical systems. *Tellus A*, **68**, 28–393.
- 479 Moran, P., 1950: Some remarks on animal population dynamics. *Biometrics*, **6**, 250–258.
- 480 Palmer, T. N., and Coauthors, 2004: Development of a European multi-model ensemble system  
481 for seasonal to inter-annual prediction (Demeter). *Bull. Amer. Meteorol. Soc.*, **85**, 853–872, doi:  
482 <http://dx.doi.org/10.1175/BAMS-85-6-853>.
- 483 Raftery, A., T. Gneiting, F. Balabdaoui, and M. Polakowski, 2005: Using Bayesian model averaging  
484 to calibrate forecast ensembles. *Mon. Wea. Rev.*, **133**, 1155–1174.
- 485 Rajagopalan, B., U. Lall, and S. E. Zebiak, 2002: Categorical climate forecasts through regular-  
486 ization and optimal combination of multiple GCM ensembles. *Mon. Wea. Rev.*, **130**, 1792–1811.
- 487 Read, P. L., 1992: *Rotating Annulus Flows and Baroclinic Waves*, 185–214. Springer Vienna,  
488 Vienna.
- 489 Ricker, W., 1954: Stock and recruitment. *J. Fisheries Res. Board Can.*, **11**, 559–623.
- 490 Roulston, M., and L. Smith, 2002: Evaluating probabilistic forecasts using information theory.  
491 *Mon. Wea. Rev.*, **130**, 1653–1660.
- 492 Roulston, M., and L. Smith, 2003: Combining dynamical and statistical ensembles. *Tellus A*, **55**,  
493 16–30.
- 494 Silverman, B., 1986: *Density Estimation for Statistics and Data Analysis*. 1st ed., Chapman and  
495 Hall, London.
- 496 Smith, L., 1992: Identification and prediction of low-dimensional dynamics. *Physica D*, **58**, 56–  
497 76.

498 Smith, L., and I. Gilmour, 1998: Enlightenment in shadows. *Nonlinear Dynamics and Stochastic*  
499 *Systems Near the Millennium*, J. B. Kadtko, and A. Bulsara, Eds., Vol. 411, AIP Conference  
500 Proceedings, American Institute of Physics, New York, United States, 201–213.

501 Smith, L. A., H. Du, E. B. Suckling, and F. Niehörster, 2015: Probabilistic skill in ensemble  
502 seasonal forecasts. *Quart. J. Roy. Meteor. Soc.*, **141**, 1085–1100.

503 Sprott, J., 2003: *Chaos and time-series analysis*. Oxford University Press, Oxford.

504 Taylor, K. E., R. J. Stouffer, and G. A. Meehl, 2012: An overview of cmip5 and the experimental  
505 design. *Bull. Amer. Meteor. Soc.*, **93**, 485–498.

506 Wang, X., and C. Bishop, 2004: Improvement of ensemble reliability with a new dressing kernel.  
507 *Quart. J. Roy. Meteor. Soc.*, **131**, 965–986.

508 Weigel, A. P., M. A. Liniger, and C. Appenzeller, 2008: Can multi-model combination really  
509 enhance the prediction skill of probabilistic ensemble forecasts? *Quart. J. Roy. Meteor. Soc.*,  
510 **134**, 241–260.

511 Weisheimer, A., and Coauthors, 2009: Ensembles: A new multi-model ensemble for seasonal-  
512 to-annual predictions—skill and progress beyond demeter in forecasting tropical pacific ssts.  
513 *Geophysical Research Letters*, **36 (21)**.

514 Wilks, D., 2006: Comparison of ensemble-mos methods in the lorenz 96 setting. *Meteorol. Appl.*,  
515 **13**, 243–256.

516 Wilks, D., and T. Hamill, 2007: Comparison of ensemble mos methods using gfs reforecasts. *Mon.*  
517 *Wea. Rev.*, **6**, 2379–2390.

518 **LIST OF FIGURES**

519 **Fig. 1.** Estimates of the Global Lyapunov exponent are plotted as a function of  $\lambda$ . a) 4096 values of  
520  $\lambda$  uniformly random sampled between 2.95 and 3.05; b) 4096 values of  $\lambda$  uniformly random  
521 sampled between 2.999 and 3.001. . . . . 29

522 **Fig. 2.** Graphical presentation of the dynamics of four different models, the blue line represents  
523 model dynamics as a function of initial conditions and the red line represents the system  
524 dynamics. . . . . 30

525 **Fig. 3.** Histogram of the 1-step model errors, given 2048 different initial conditions with respect to  
526 natural measure. . . . . 31

527 **Fig. 4.** Graphical presentation of the 2-step evolution of four different models, the blue line repre-  
528 sents the 2-step model evolution as a function of initial conditions and the red line represents  
529 the 2-step evolution under the system. . . . . 32

530 **Fig. 5.** Histogram of the 2-step model errors, given 2048 different initial conditions with respect to  
531 natural measure. . . . . 33

532 **Fig. 6.** a) The best found perturbation parameter values  $\kappa$  as a function of lead time for each model,  
533 the dashed black line reflects the standard deviation of the noise model. b) Ignorance score  
534 of each model as a function of lead time, the dashed black line reflects skill of climatology  
535 which defines zero skill. . . . . 34

536 **Fig. 7.** The Ignorance score varies as the ensemble size increases for each model. . . . . 35

537 **Fig. 8.** Forecast Ignorance, climatology-blend weight assigned to the model, kernel width and  
538 weights assigned to each individual model are plotted as a function of lead time. . . . . 36

539 **Fig. 9.** Climatology-blend weights assigned to each model. The red bars are the 95<sup>th</sup> percentile  
540 range of the fitted weights based on 512 forecast-outcome archives. Each contains 2048  
541 forecast-outcome pairs. The blue crosses represent the histogram of the fitted weights based  
542 on 512 forecast-outcome archives. Each of these contains only 40 forecast-outcome pairs. . . . 37

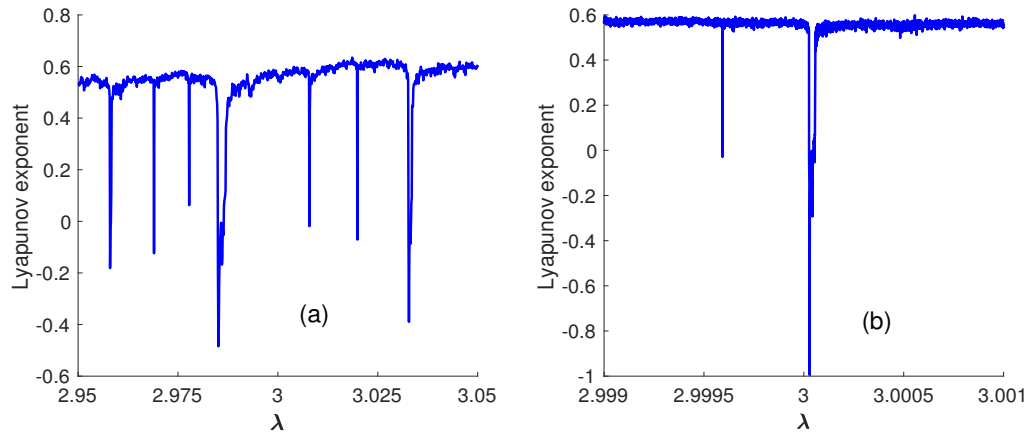
543 **Fig. 10.** Kernel width of each model’s forecasts. The red bars are the 95<sup>th</sup> percentile range of the  
544 fitted kernel width based on 512 forecast-outcome archives, each contains 2048 forecast-  
545 outcome pairs. The blue crosses represent the histogram of the fitted kernel width based on  
546 512 forecast-outcome archives, each contains only 40 forecast-outcome pairs. . . . . 38

547 **Fig. 11.** Ignorance score of each model’s forecasts. The red bars are the 95<sup>th</sup> percentile range  
548 of Ignorance score calculated based on a testing set containing 2048 forecast-outcome  
549 pairs, using the climatology-blend weights and kernel widths fitted based on 512 forecast-  
550 outcome archives, each contains 2048 forecast-outcome pairs. The blue crosses represent  
551 the histogram of Ignorance score calculated based on the same testing set but using the  
552 climatology-blend weights and kernel widths based on 512 forecast-outcome archives, each  
553 contains only 40 forecast-outcome pairs. . . . . 39

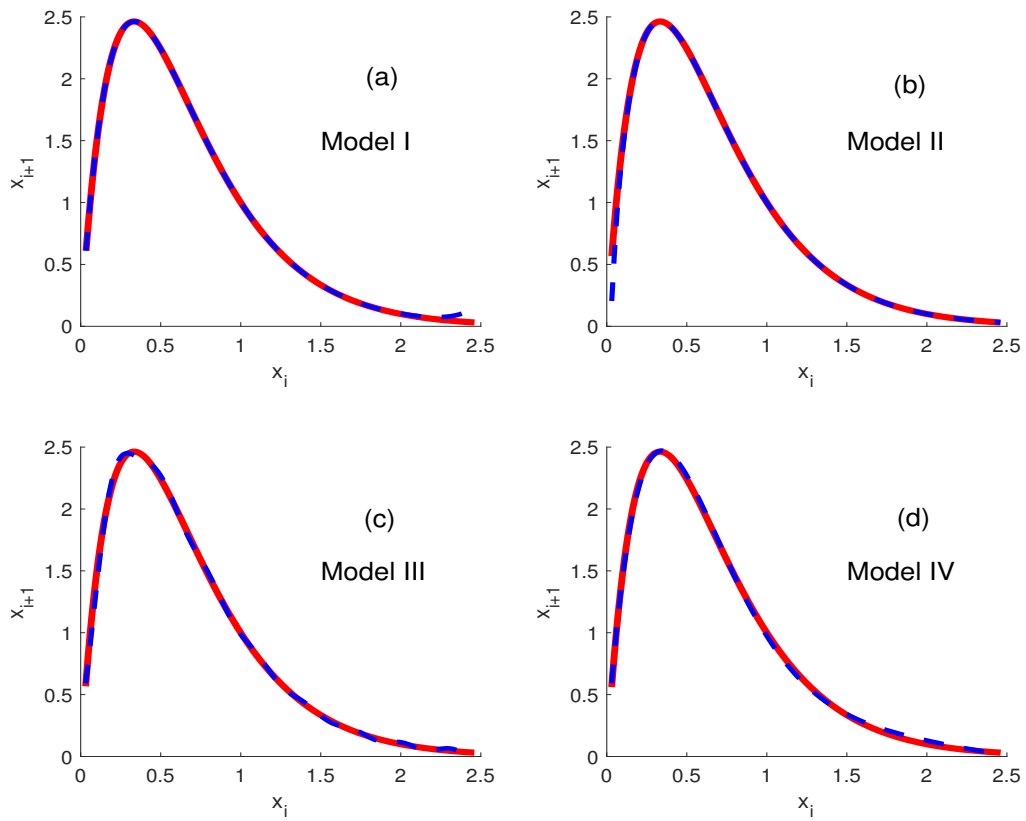
554 **Fig. 12.** Multi-model weights for each set of model forecasts. The red bars are the 95<sup>th</sup> percentile  
555 range of model weights calculated based on a testing set containing 2048 forecast-outcome  
556 pairs, using the climatology-blend weights and kernel widths fitted based on 512 forecast-  
557 outcome archives, each contains 2048 forecast-outcome pairs. The blue crosses represent  
558 the histogram of model weights calculated based on the same testing set but using the

559 climatology-blend weights and kernel widths based on 512 forecast-outcome archives, each  
560 contains only 40 forecast-outcome pairs. . . . . 40

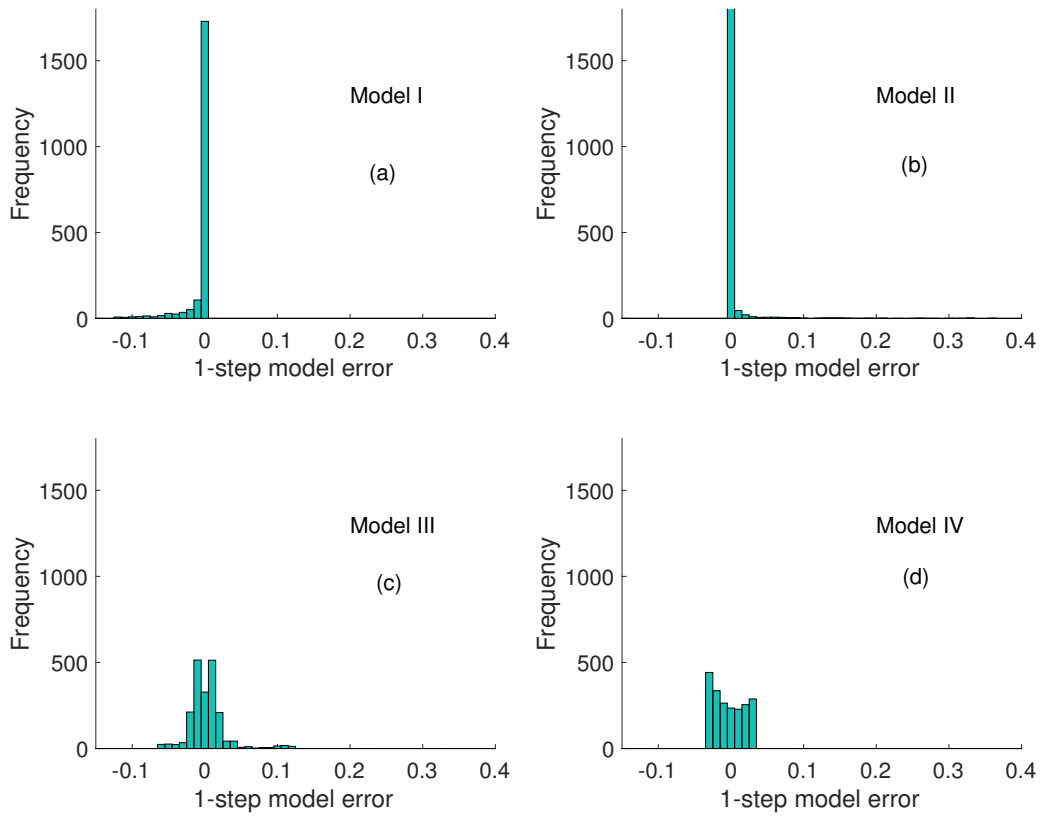
561 **Fig. 13.** Ignorance of multi-model ensemble relative to the single best model. The blue crosses rep-  
562 resent the histogram of the Ignorance of the multi-model ensemble relative to the single best  
563 model (black dashed line). (a) Model weights and dressing and climatology-blend parame-  
564 ters are fitted based on 512 large archives, each contains 2048 forecast-outcome pairs. (b)  
565 Model weights and dressing and climatology-blend parameters are fitted based on 512 small  
566 archives, each contains 40 forecast-outcome pairs. (c) The Ignorance of the multi-model  
567 ensemble is calculated using model weights and dressing and climatology-blend parameter  
568 which are fitted based on 512 small archives, while the Ignorance of the single best model  
569 is calculated based on 512 large archives. . . . . 41



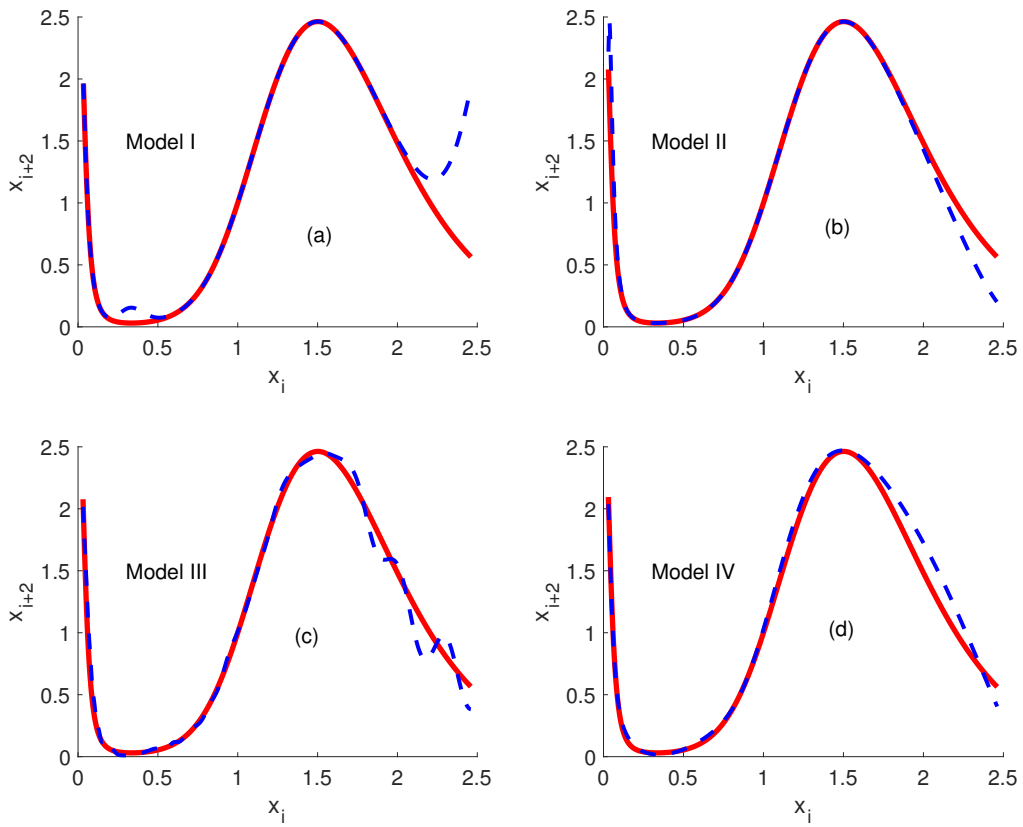
570 FIG. 1. Estimates of the Global Lyapunov exponent are plotted as a function of  $\lambda$ . a) 4096 values of  $\lambda$   
 571 uniformly random sampled between 2.95 and 3.05; b) 4096 values of  $\lambda$  uniformly random sampled between  
 572 2.999 and 3.001.



573 FIG. 2. Graphical presentation of the dynamics of four different models, the blue line represents model  
 574 dynamics as a function of initial conditions and the red line represents the system dynamics.

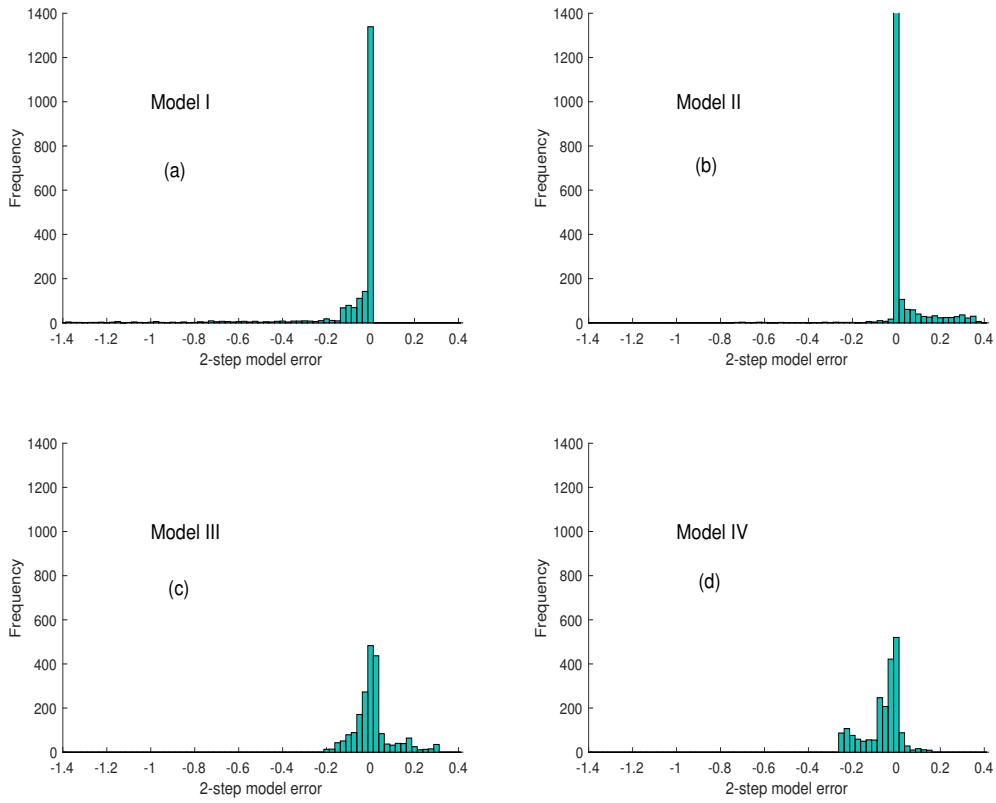


575 FIG. 3. Histogram of the 1-step model errors, given 2048 different initial conditions with respect to natural  
 576 measure.

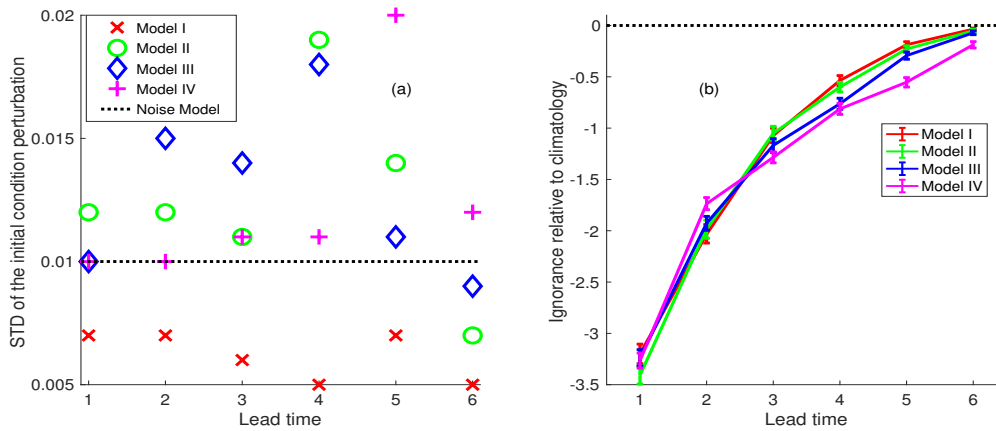


577 FIG. 4. Graphical presentation of the 2-step evolution of four different models, the blue line represents the  
 578 2-step model evolution as a function of initial conditions and the red line represents the 2-step evolution under  
 579 the system.





580 FIG. 5. Histogram of the 2-step model errors, given 2048 different initial conditions with respect to natural  
 581 measure.



582 FIG. 6. a) The best found perturbation parameter values  $\kappa$  as a function of lead time for each model, the  
 583 dashed black line reflects the standard deviation of the noise model. b) Ignorance score of each model as a  
 584 function of lead time, the dashed black line reflects skill of climatology which defines zero skill.

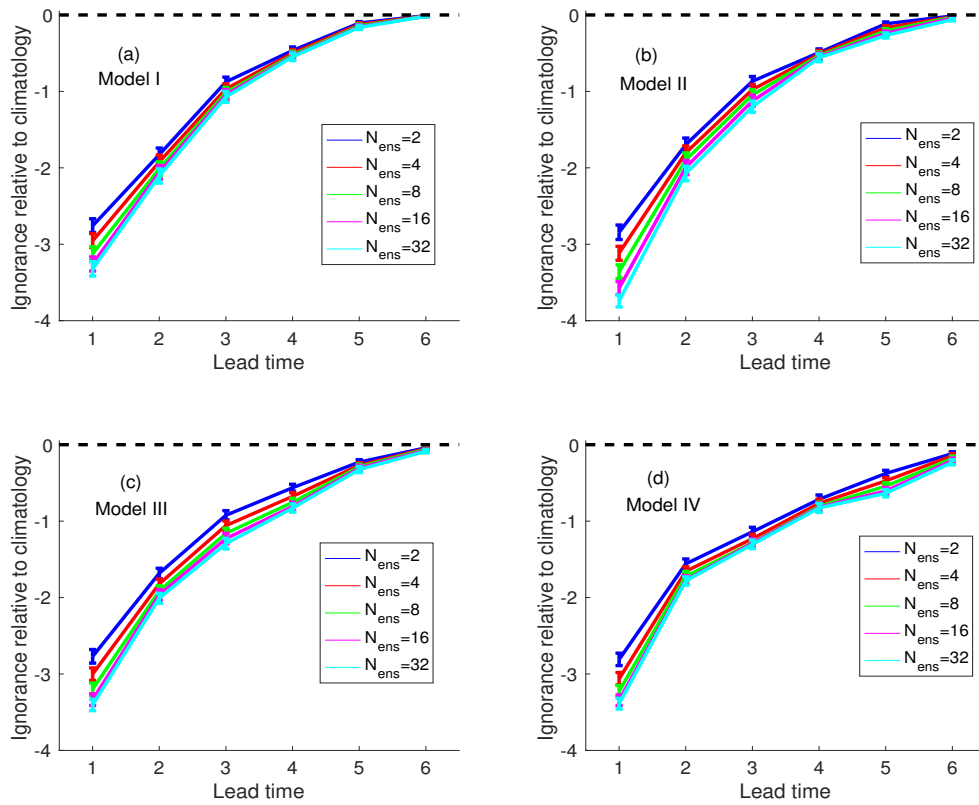
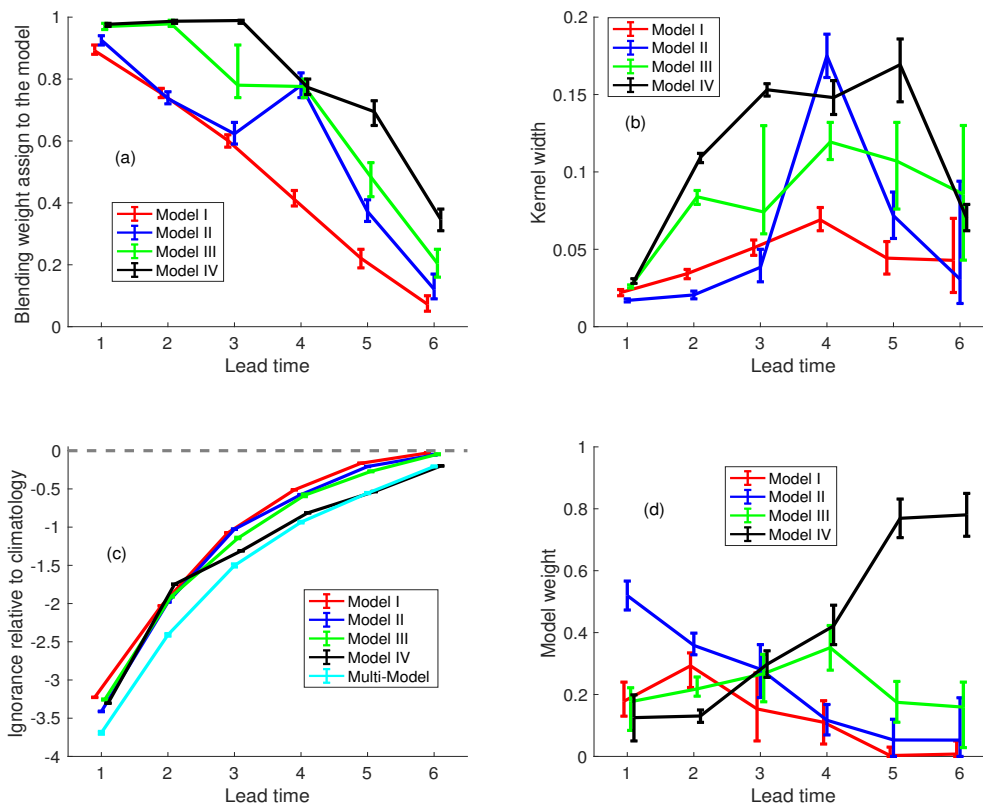
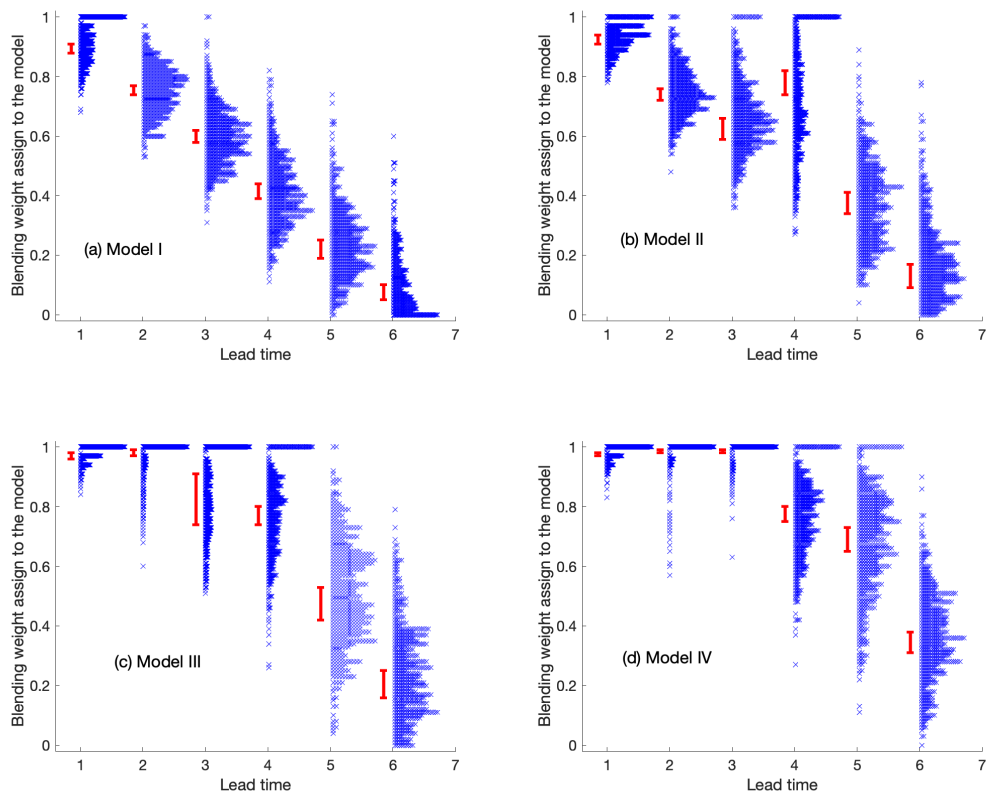


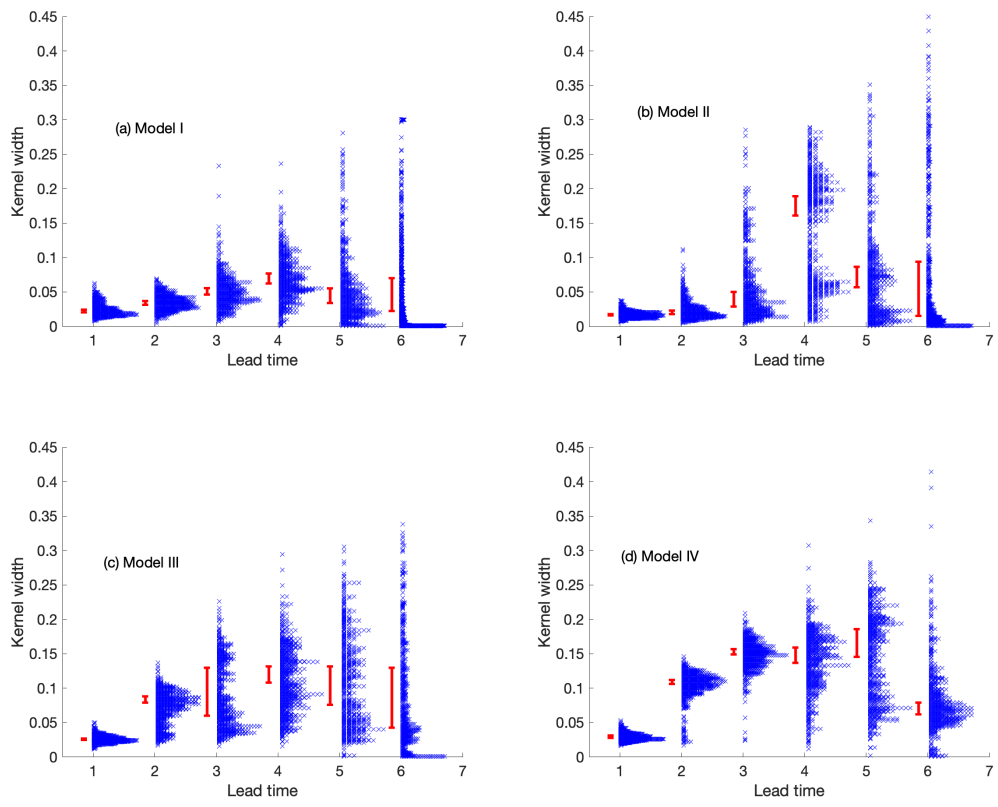
FIG. 7. The Ignorance score varies as the ensemble size increases for each model.



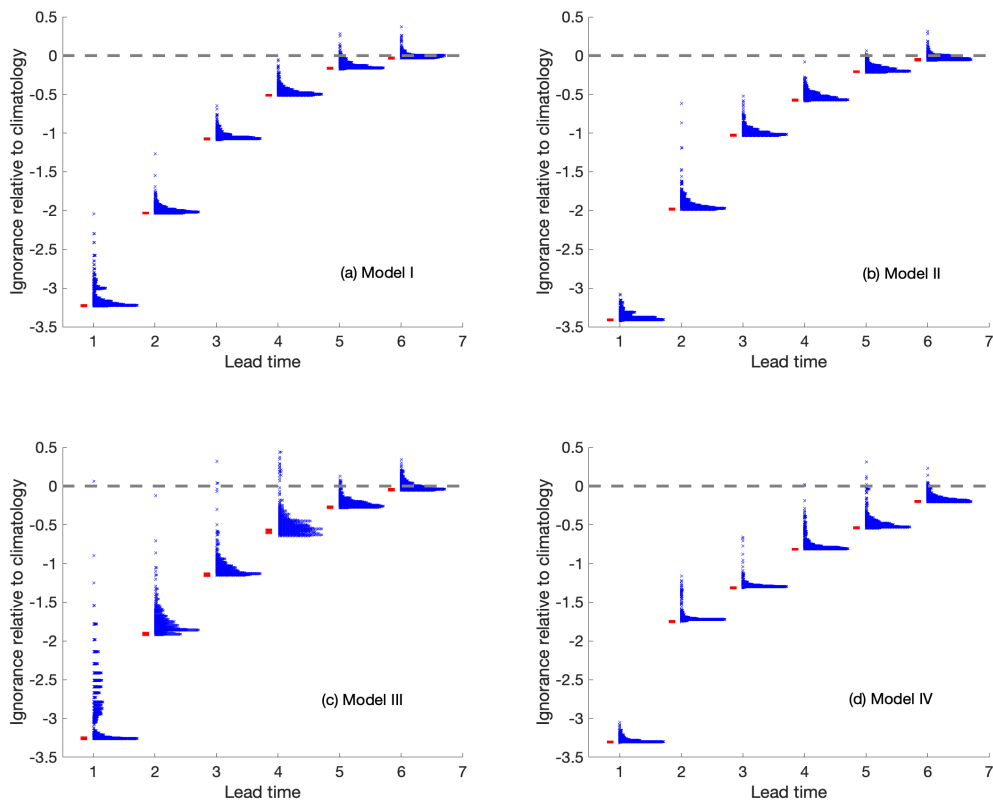
585 FIG. 8. Forecast Ignorance, climatology-blend weight assigned to the model, kernel width and weights as-  
 586 signed to each individual model are plotted as a function of lead time.



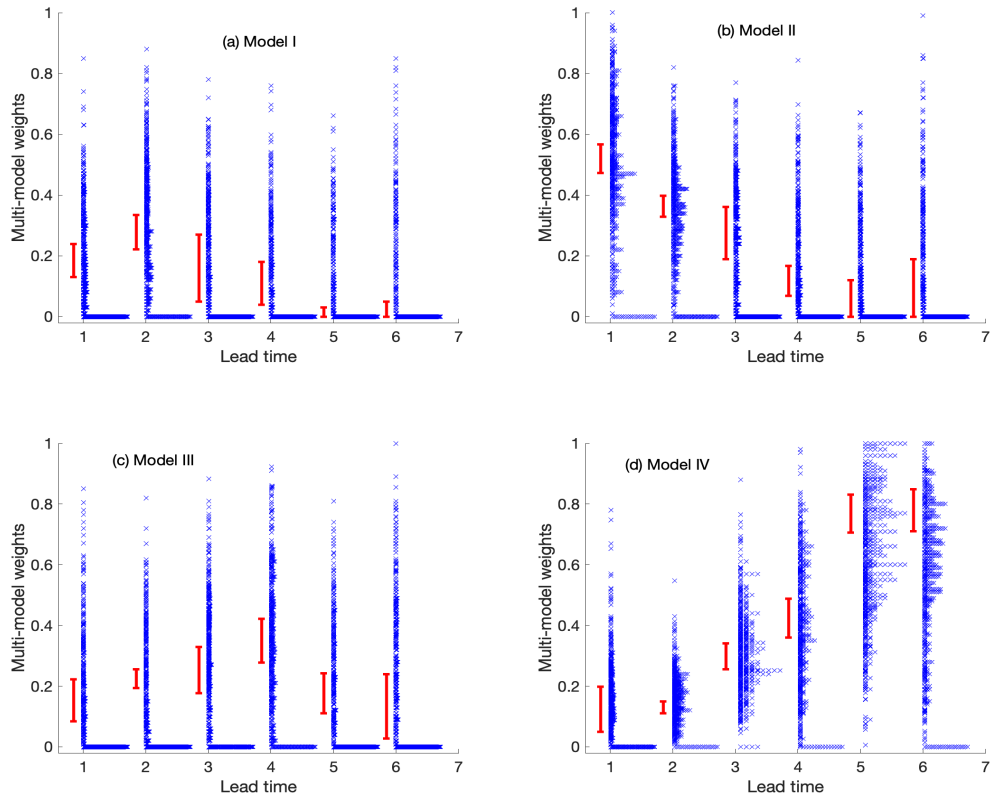
587 FIG. 9. Climatology-blend weights assigned to each model. The red bars are the 95<sup>th</sup> percentile range of the  
 588 fitted weights based on 512 forecast-outcome archives. Each contains 2048 forecast-outcome pairs. The blue  
 589 crosses represent the histogram of the fitted weights based on 512 forecast-outcome archives. Each of these  
 590 contains only 40 forecast-outcome pairs.



591 FIG. 10. Kernel width of each model's forecasts. The red bars are the 95<sup>th</sup> percentile range of the fitted kernel  
 592 width based on 512 forecast-outcome archives, each contains 2048 forecast-outcome pairs. The blue crosses  
 593 represent the histogram of the fitted kernel width based on 512 forecast-outcome archives, each contains only  
 594 40 forecast-outcome pairs.

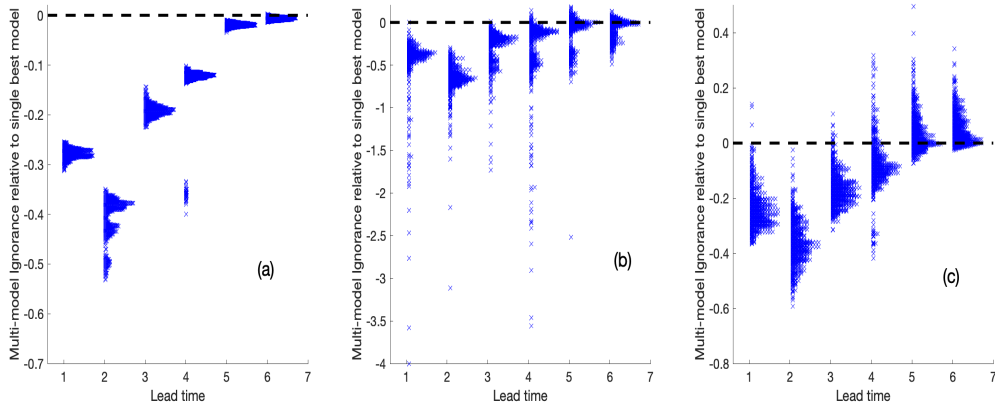


595 FIG. 11. Ignorance score of each model's forecasts. The red bars are the 95<sup>th</sup> percentile range of Ignorance  
 596 score calculated based on a testing set containing 2048 forecast-outcome pairs, using the climatology-blend  
 597 weights and kernel widths fitted based on 512 forecast-outcome archives, each contains 2048 forecast-outcome  
 598 pairs. The blue crosses represent the histogram of Ignorance score calculated based on the same testing set but  
 599 using the climatology-blend weights and kernel widths based on 512 forecast-outcome archives, each contains  
 600 only 40 forecast-outcome pairs.



601 FIG. 12. Multi-model weights for each set of model forecasts. The red bars are the 95<sup>th</sup> percentile range of  
 602 model weights calculated based on a testing set containing 2048 forecast-outcome pairs, using the climatology-  
 603 blend weights and kernel widths fitted based on 512 forecast-outcome archives, each contains 2048 forecast-  
 604 outcome pairs. The blue crosses represent the histogram of model weights calculated based on the same testing  
 605 set but using the climatology-blend weights and kernel widths based on 512 forecast-outcome archives, each  
 606 contains only 40 forecast-outcome pairs.





607 FIG. 13. Ignorance of multi-model ensemble relative to the single best model. The blue crosses represent the  
 608 histogram of the Ignorance of the multi-model ensemble relative to the single best model (black dashed line).  
 609 (a) Model weights and dressing and climatology-blend parameters are fitted based on 512 large archives, each  
 610 contains 2048 forecast-outcome pairs. (b) Model weights and dressing and climatology-blend parameters are  
 611 fitted based on 512 small archives, each contains 40 forecast-outcome pairs. (c) The Ignorance of the multi-  
 612 model ensemble is calculated using model weights and dressing and climatology-blend parameter which are  
 613 fitted based on 512 small archives, while the Ignorance of the single best model is calculated based on 512 large  
 614 archives.